INTERNATIONAL JOURNAL OF
COASTAL, OFFSHORE & ENVIRONMENTAL ENGINEERING IJCOE Vol.7/No. 2/Spring 2022 (39-48)

Available online at: www. Ijcoe.org

Experimental Analysis of the Effect of a Submerged obstacle and Floating Wave Barrier in front of a Rubble Mound Breakwater on Diminishing the Damage Parameter

Ramin Vafaeipour Sorkhabi [1*], Mohammad Taghi Alami [2], Alireza Naseri[3], Alireza Mojtahedi[4]

[1] Assistant professor, Department of Civil Engineering, Tabriz Branch, Islamic Azad University, Tabriz, Iran, raminvafaei@yahoo.com*

[2] Professor, Department of Water Resources Management, Faculty of Civil Engineering, University of Tabriz, Tabriz, Iran, mtaalami@tabrizu.ac.ir

[3] Ph.D. Candidate, Water Engineering and Hydraulic Structures, University of Tabriz, Tabriz, Iran, naseri@gmx.com

[4] Associate professor, Department of Water Resources Management, Faculty of Civil Engineering, University of Tabriz, Tabriz, Iran, a.mojtahed@tabrizu.ac.ir

ARTICLE INFO

Article History:
Received: 18 Feb. 2020
Accepted: 22 May. 2022

Keywords:
Rubble mound breakwater
Random wave
Damage parameter
Submerged obstacle
Floating wave barrier

ABSTRACT

The aim of this research was to compare the performance of a submerged obstacle and floating wave barrier in the stability of rubble mound breakwaters based on the damage parameter. The submerged obstacle was attached to the toe, and the floating wave barrier was installed 50 cm from a reshaping breakwater. We carried out tests in a 35 m flume at SCWMRI. Random waves with the JONSWAP spectrum influenced the breakwater. We then analyzed the structure's reshaping using close-range photogrammetric imaging by constructing the DEM and DSM to record the displacement of rocks. Furthermore, we obtained the eroded area and the damage parameter from the integrated model at eight cross-sections at equal distances. We showed that the damage parameter increased by 39.12 and 44.44%, respectively, by increasing the relative wave height from 0.36 to 0.48 and 0.6. Also, the damage parameter increased by 22.94 and 28.26%, respectively, by increasing the relative wave period from 0.6 to 0.8 and 1. In addition, regarding different modes, we obtained the damage parameter in the breakwater without the submerged obstacle and the floating barrier 1.116 under random waves. The damage parameter decreased to 0.701 (i.e., 37.19%) by using the submerged obstacle, while the wave barrier reduced this parameter to 0.735 (i.e., 34.14%); thus, the obstacle has outperformed the wave barrier. Using the obstacle simultaneously with the wave barrier reduced the damage parameter by 51.79%, confirming the highest efficiency and performance among models. Consequently and based on the experiments and findings in this study, this model was suggested for adoption.

1. Introduction

Rubble mound breakwaters (RMBs) are used to dissipate sea wave's energy and prevent damages to facilities and shoreline areas. These structures generally involve three main layers: core, filter, and armor [1]. It has been tried to minimize the hydrodynamic forces from the waves by reshaping and launching RMBs to create a stable structure profile [2]. At present, researchers are performing numerous tests on the stability of the armor layer and the dimensions of the reshaping RMBs. Sayao & Da Silva (2016) studied the relationship between structural features such as wall slope, crest width, and breakwater height with the performance of the attacking wave [3]. In modeling, Lamberti et al. (1994) emphasized the importance of water depth at the structure's base and shallow water conditions. They showed that the final profile deformation coefficients were related to reflection depth, wave sharpness, and floor slope in addition to wave height [4]. In the design and construction of breakwaters, it is vital to reduce the waves' energy and not be destroyed by the waves. RMB

damage indicates demolition of the structure and hydraulic instability against the waves [5]. Thus, modeling the damage progression and investigating the representative parameters of this process for boosting the performance and lifespan of the breakwater seems essential. Campos et al.(2020), noting the complexity of the progression of damage in the Armor layer due to the random nature of the impact of the waves, considered it very useful and essential to monitor the structure's performance by accurate imaging techniques [6]. By examining the stability of RMBs in terms of breaking similarity parameter, Sayao (1998) evaluated the permeability of the structure as an essential factor in the hydraulic stability of the structure [7]. Dimensions of the rocks used in breakwater are related to the armor damage level in the face of the waves. In experiments, Rao and Pramod (2003) showed that as the size of the rocks decreases, the amount of damage to them increases [8]. In another study, Panagiota et al. (2018) also assessed that the leading cause of failure of conventional RMBs was mainly due to damage to the armor layer or scouring of the structural toe or upward and overflow of waves [9]. Researchers have considered selecting crucial variables to reduce the number of experiments without affecting the results in estimating breakwater damage levels. Researchers such as Janardhan et al. (2015) have used various methods, such as Principal Components Regression (PCR) [10].

The use of submerged breakwaters is also one of the new solutions against coastal erosion. Wave breaking by submerged breakwaters brings about turbulence at the toe of the RMB. Friction resistance and turbulence increase the energy dissipation due to decreasing wave reflection and bed scouring, thus adjusting the sediments [1]. Also, Twu et al. (2001) considered wave transmission, wave run-up, and wave motion changes in submerged breakwaters [11]. Neves et al. (2007) observed that the permeability of submerged breakwaters affects the flow characteristics caused by the waves and reduces the horizontal flow velocity [12]. It is also possible to reduce the wave energy by applying submerged obstacles. In a laboratory study, Bungin (2021) used a set of 5 cm cubes with a distance of 1.1 cm in a 100 and 200 cm path as a submerged breakwater and observed that the wave height decreased by 60 to 80% [13]. In addition to protecting the existing breakwater, submerged breakwaters protect shorelines and the facilities. These structures are used for reconstructing the damaged or destroyed RMBs [14]. In a study, Tulsi and Phelp (2009) examined the effect of a submerged breakwater on protecting the crown of a damaged RMB. They found that the submerged structure could break and debilitate the storm waves, save the damaged part of the RMB, and ultimately repair the main RMB [15]. Given the behavior of the submerged obstacle, its application as a structure alongside the RMB seems appropriate. Constructors use precise and essential information such as wave characteristics and structural properties to design this composite structure. It is believed that boosting the breakwaters' optimal performance is viable by modifying the dimensions, wall slope, and position of the submerged structure [16]. In a project, the Stefanutti Stocks (2015) reduced the weight characteristics of the breakwater armor layer by designing a set of the submerged breakwaters to decrease the waves and protect the RMB near the coast [17].

Researchers have always considered innovative methods. For example, He et al. (2012) investigated the combination of pneumatic and submerged breakwaters by considering multiple slope front breakwater based on experimental and numerical models to find the optimal slope [18]. The numerical modeling results by Jian Xu et al. (2020) to analyze the combined effect of submerged and pneumatic breakwaters in reducing the energy of the waves showed a significant increase in energy dissipation capacity by up to 35% compared to the single breakwater [19]. In another study, Qin et al. (2019) numerically modeled submerged breakwaters in one and two rows in the face of regular waves using the fluid-structure interaction (FSI) algorithm and evaluated the second row of breakwaters' use effective [20]. We should know that even in critical situations, using a submerged structure idea next to a RMB is considered. In a project, Quiroga et al. (2018) investigated the effect of using RMB to deal with tsunami waves. Their experiments determined the values of the damage parameter used to describe the damage (onset of damage, onset of destruction, and complete demolition) during a tsunami [21].

This paper is an experimental study highlighting the impacts of a submerged obstacle and a floating wave barrier in front of a RMB using the damage parameter. Therefore, we connected the submerged obstacle to the structure and placed the floating wave barrier at a distance of 50 cm. Under the influence of random waves, we obtained and compared the damage number.

2. Materials and methods

The submerged obstacle in front of the toe prevents rocks from falling, and it acts as a support. The rock fall and the dependence on the submerged obstacle reduce the demolition process, contributing to the RMB stabilization in a smaller area, consequently diminishing the damage parameter. The wave force is the main factor on the RMB, making the breakwater reshape and collapse; decreasing the wave force would reduce its destructive energy by the second power of the wave height. Consequently, the floating wave barrier that resists the waves and reduces their height would be capable of downgrading its destructive power leading to decreased damage parameter. Therefore, comparing the submerged obstacle and the floating wave barrier or their combined effect is of tremendous importance.

2.1. Test procedure

The present experimental study explores the influence of a submerged obstacle attached to the toe and a floating wave barrier at a distance of 50 cm from it on the wave stability of the RMB. In this paper, the toe-connected submerged obstacle is referred to as an obstacle, the floating wave barrier laid at a distance of 50 cm from the RMB, called the wave barrier. Literature review shows that RBM stability has been studied primarily in the lateral or middle sections of the structure. However, the current study applied close-range photogrammetric imaging for providing dense cloud and a combined integrated 3D model of various height elevations to develop a detailed RMB model before and following the wave attacks. In the close-range photogrammetric imaging, the images taken from a close distance were put to analysis for obtaining a reshaped RMB model that could pinpoint the displacement at any point accurately. Since the RMB profile upon encounter with waves did not follow a regular change trend along with the structure, and it constantly changed, some unpredicted changes occur. This issue complicates studies. Well-documented and accurate data leads to better research results contributing to precise measurement of the RMB displacement of armor rocks upon encounter with waves. This method is not destructive and has no adverse effects, and it offers real-time 3D measurements with higher accuracy and speed. In addition, the waves produced by the wave maker were based on the JONSWAP spectrum, which was selected because of its high spectral energy, and in the absence of a field spectrum for laboratory studies can be one of the most appropriate spectra.

2.2. Environmental and structural governing variables

A range of governing variables and non-dimensional characteristics used in this study are listed in Tables 1 and 2. It is believed that wave steepness is the crucial issue to consider for choosing the height and period of the wave. It is essential to take the wave height and period into account to be placed the wave steepness generated by combining the two parameters to stand in the 0.015 to 0.07 range [22]. A combination of wave height and period at a steepness range of 0.01 to 0.054 has been suggested in some studies [23, 24]. The wave height was set to range from 4 to 15 cm based on the laboratory facilities, depth, and the type of wave maker conditions because it is viable to observe scale effects in waves having less than 4 cm height. However, turbulence at the surface of generated waves is expected by the waves with a higher height level at the paddle-generated wave due to large displacements, thus perplexing the accuracy of the data collected. This paper only examined the non-breaking waves. It showed that when the significant wave height surpassed 15 cm during the experiment, the wave could break before striking the breakwater.

Table 1. Range of governing variables

Variable	Expression	Range
Wave height [*cm*]	H_s	9, 12, 15
Wave period [*s*]	T_p	0.9, 1.2, 1.5
Storm duration (Zero up-crossing method)	N	3000
Nominal diameter [*cm*]	D_{n50}	1.7
Mass density [gr/cm^3]	ρ	2.55
Water depth [*cm*]	d_i	25
Slope of breakwater	cot α	1.25
Slope of submerged	cot α_1	1.25

Table 2. Non-dimensional characteristics

Variable	Expression	Range
Ratio of the thickness of armor layer to the nominal diameter	t_A/ D_{n50}	15
Armor material gradation	D_{n85A}/ D_{n15A}	1.82
Wave steepness	s_{om}	0.01 to 0.07
Relative crest width of submerged	B/d	0.4
Relative height of submerged	h/d	0.32

2.3. Wave flume

The tests were done in a 35 m long, 5 m wide, and 1 m deep flume at Soil Conservation and Watershed Management Research Institute (SCWMRI); its features are illustrated in Figures 1 and 2. The wave flume was separated into three parts by two walls of 24.5 meters long and 1 meter high to avoid transverse waves. The waves were produced by a vertical piston generator arm of 5.5 m length and 1 m height positioned at the end of the flume. This wave maker could generate regular and random waves of different spectrums regular and randomly.

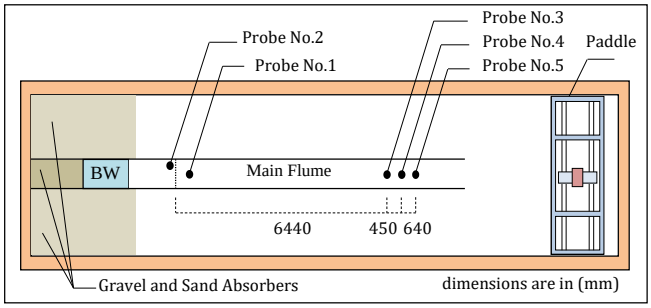

Figure 1. Sketch of wave flume and position of the RMB structure and wave probes

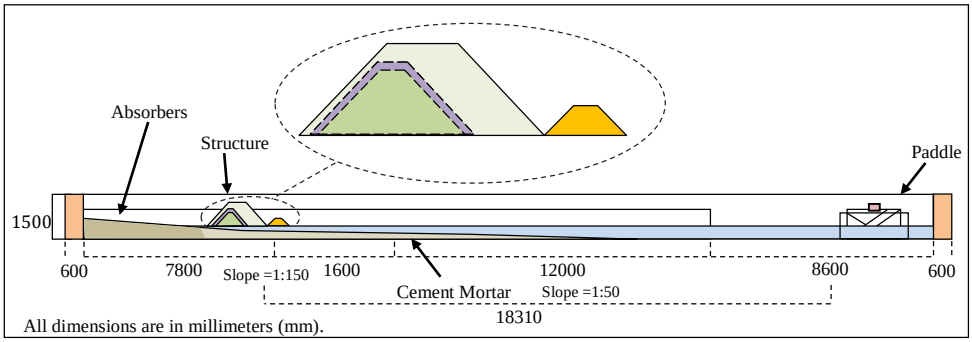

Figure 2. Transversal section of the wave flume and the position of the RMB and the obstacle

The waves generated and used in all experiments were random based on the JONSWAP spectrum. Five wave probes were applied in the flume to log variations of the water surface height with one-millimeter accuracy.

2.4. Breakwater model

The breakwater with a uniform slope of 1V:1.25H is constructed on the flatbed of the flume with primary stone armour of nominal diameter D_{n50} equal to 1.7 cm. A stable obstacle of 80 mm height is designed with plexiglass. The slope of the obstacle is 1V:1.25H, uniformly installed seaward of the RMB. The obstacle is filled with heavy material to submerge entirely and to behave steadier against the waves. Moreover, a wave barrier with dimensions of 100 mm is designed with plexiglass; the weight of this barrier is precisely adjusted to submerge in the water to half of its depth (with 50% immersion) while being held to the flume bed by a wired cable. The white anti-reflective fabric is applied to cover the obstacle to avoid light reflection and errors in imaging and capture the location of points and profiles. The features of RMB, obstacle, and

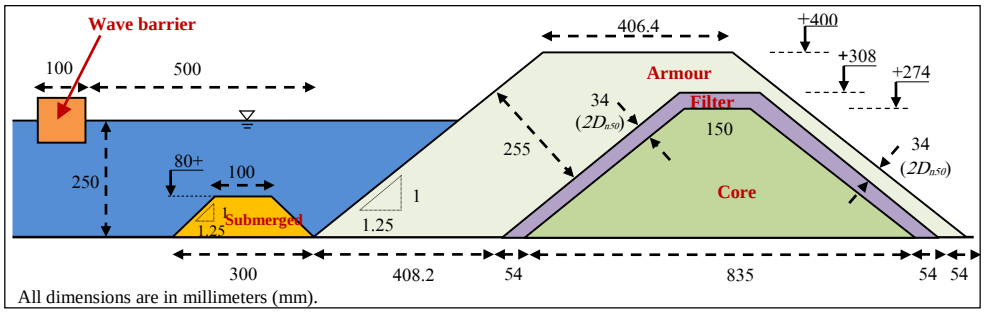

Figure 3. Dimensions and distances of the RMB, obstacle, and wave barrier

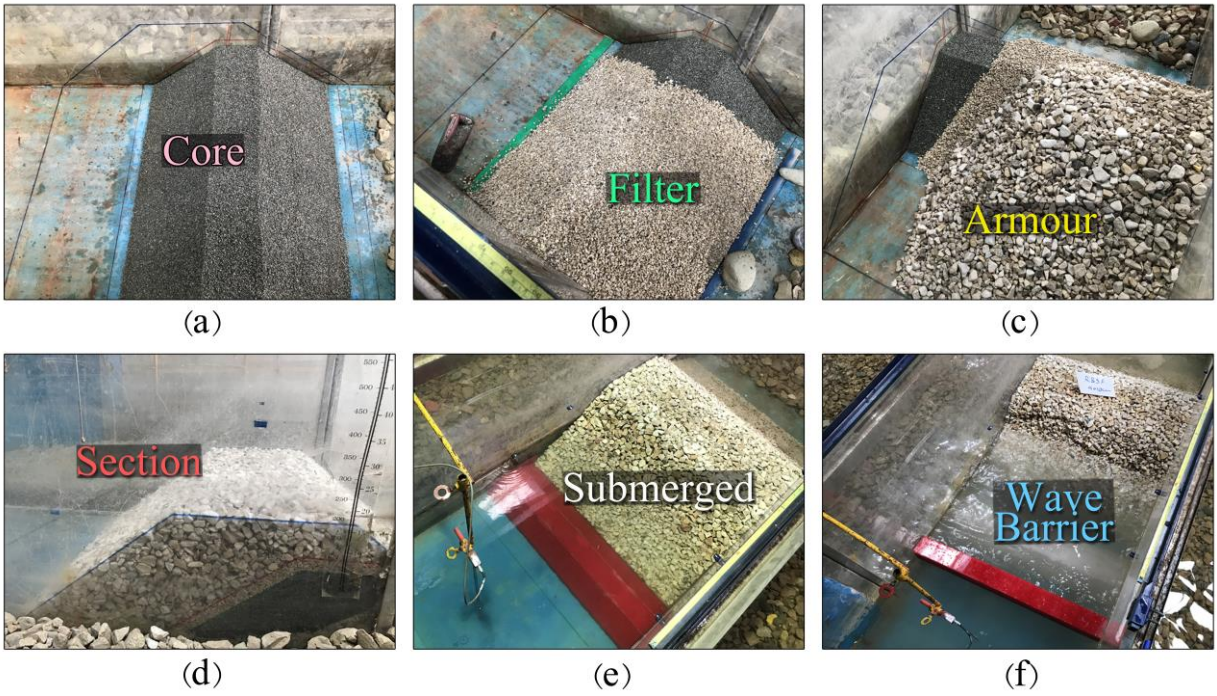

Figure 4. (a) core, (b) filter, (c) armour, (d) Transversal section of the RMB, (e) obstacle, (f) wave barrier

barrier, are shown in Figure 3 and their images in the fabrication and experiment phases in Figure 4.

2.5. Measurements and Data interpretation

Before performing tests, the experimental setup was calibrated and controlled. Some assumptions were also taken into account in tests, e.g., secondary waves in the wave generation process are not considered, flume bed is the horizontal, merely hydraulic performance of the model is considered, and Wave reflection from the breakwater does not encounter with newly generated waves [25]. For making the 3D model, 11 points were first marked on the flume by recording the coordinates of the breakwater range using a surveying camera. Then, before and following tests (or after a certain number of waves), the breakwater was photographed with a professional camera; afterward, images were transferred to software, processed, and digitized to produce photo blocks. Finally, the Digital Elevation Model (DEM) and Digital Surface Model (DSM) were prepared. Some properties of the integrated 3D model specified by the software listed in Table 3.

Table 3. Specifications of the 3D model

Aligned Cameras	GCP (Markers)	Dense Point Cloud	Tie Points	Flying Altitude (m)	Coverage Area (m^2)
27	11	2073622	20471	1.13	2.28

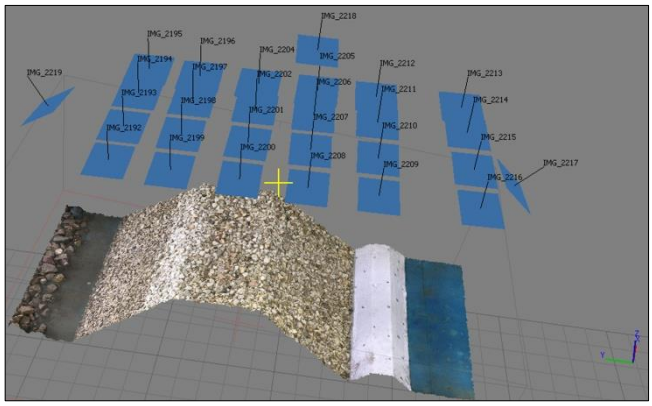

Figure 5. Position of markers and cameras from the RMB

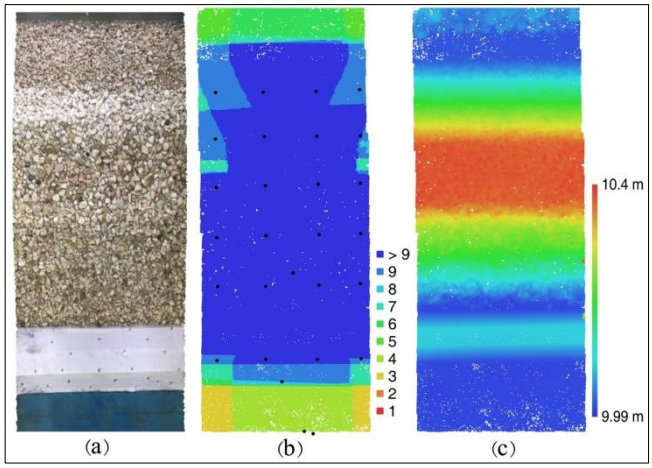

Figure 6. (a) Integrated images, (b) images overlaps, (c) DEM

Images of the structure surface were taken at regular intervals. Around 25 to 27 images were prepared for each test segment and transferred to the software to develop a 3D model. Sample of markers and pictures taken from the breakwater in the AGISOFT is clear from Figure 5. In addition, Figure 6(a) shows a set of images taken, and Figure 6(b) displays the image overlaps; Figure 6(c) demonstrates the DEM.

3. Results and Discussion

Analyzing the test results using the main parameters is an essential issue for studying RMB hydraulic stability.

3.1. Random wave

The wave paddle is of the piston type. The wave maker could produce regular and random waves under the Bretschneider, Pierson-Moskowitz, and JONSWAP spectrum, with the maximum height of generated wave standing at 20 cm. The wave probes are based on resistance detectors, and they could accurately measure the water surface fluctuations regarding the static water surface. The wave height was obtained for every solo wave using the time series harvested via the zero up-crossing methods. In this method, the wave intercepts with the reference line (water surface elevation) in two points. The wave height is the maximum difference of water surface elevation between two solid points and the wave period is the time interval from the first solid point to the second one [26]. Accordingly, a code was prepared in MATLAB and used water surface time series to differentiate the waves and provide the height and periods of the individual waves. The maximum height, significant wave height, average wave height, maximum period, significant wave period, average period, wavelength, and frequency were calculated from the resultant height and periods. The JONSWAP spectrum and the experimental spectra are shown in Figure 7. Based on the results, the wave height and period through the zero up-crossing results do not match the observed values. However, from among the three mean, significant, and max wave heights and periods, the significant mode was closer to the height and period of the wave maker. This case can also be observed in both the JONSWAP spectrum created by the wave maker at the water surface and the results of the wave separation code. For example, considering the wave height of 12 cm defined for the wave maker, the wave heights under mean, significant, and maximum mode were 5.3, 11.38, and 15.59 cm, respectively. All performed tests verified this finding.

Consequently, the height and period defined for the wave maker can be approximated as the significant height and period. The number of waves generated from the water surface was also lower than the expected figure. For example, at a wave height of 12 cm, a period of 1 second, and a duration of 5400 seconds (1.5 hours), 5400 single waves were expected to be generated, while the zero up-crossing method results would offer 5173 waves. This reduction happens because the water surface transfers to the next wave without cutting the

zero level in tiny waves. That wave is being practically eliminated in counting the waves. According to tests, the discrepancy between these two numbers regarding the effect of the number of waves on the RMB reshaping was not significant as it was controlled for experiments.

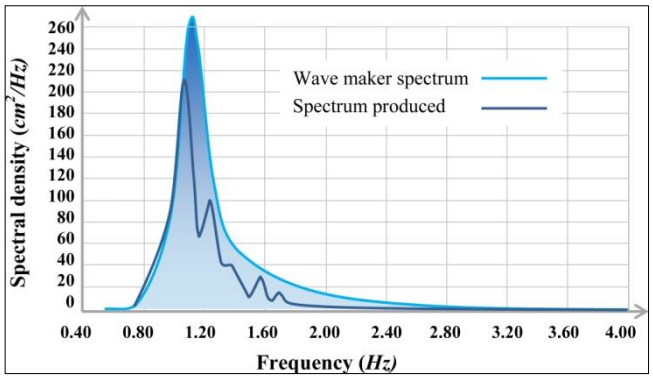

Figure 7. JONSWAP spectrum and experimental spectra

3.2. Reshaping profiles

At the beginning of the experiments, RMB (as the control test) was subjected to random waves for observing the performance of the obstacle and the wave barrier accurately. Moreover, the reshaping of armor in different heights and periods was studied so that the controlled structure against the waves would determine the damage to the RMB realistically and accurately. By the damage parameter, it is meant: ($S=\frac{Ae}{D_{n50}^2}$), Where A_e is the eroded area and D_{n50} the nominal diameter of the armor layer. The reshaping of the armor rocks and the final profile of the structure is depicted in Figure 8. The level of displaced material as the average value (average variations in 8 bands) is shown in Figure 9. Figure 10 shows a DEM of the breakwater and a transversal section through the middle of the structure. Also, a side view of the section before and after the test is shown in the figure. Since numerous images are available, the shapes were not repeated for all tests in

Figure 8. Top view, side view, and bird's-eye view before and after the test

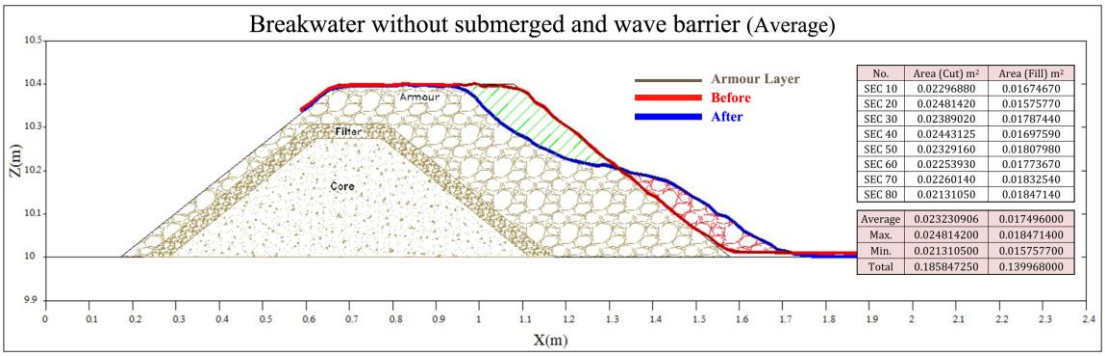

Figure 9. Average area of displaced rocks and profile reshaping

this study.

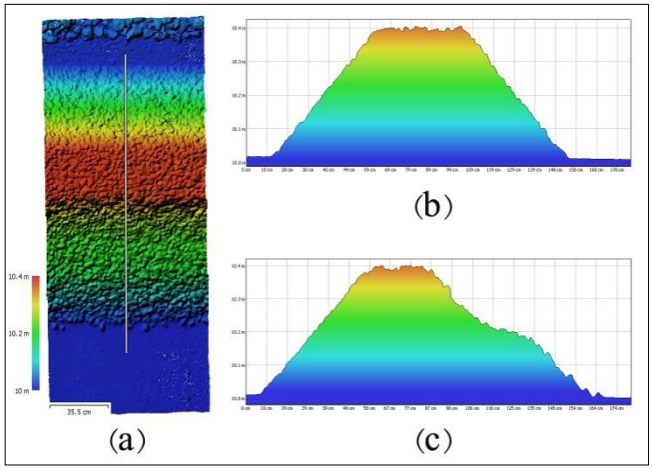

Figure 10. (a) DEM and transversal section (b) Selected section before the test (c) Selected section after test

3.3. The effect of wave characteristics on RMB reshaping

Following the tests, height, period, and the number of waves (storm duration) parameters were assessed as the primary characteristics influencing the structure's stability and monitoring the erosion when the obstacle was connected to the RMB. For studying the stability trend, the RMB was tested at the height of 12 cm and a period of 1 second with several incident waves ranging from 1000 to 6000. Results are demonstrated in Figure 11. The damage parameter was calculated by S ($S=\frac{Ae}{D_{n50}^2}$) for each test; as shown, the maximum profile change (over 50%) happened when the first 1000 waves hit, and the erosion of the armor layer followed an increasing trend up to 3000 waves; the erosion pace significantly decreasing between 3000 and 4000 waves. Note that erosion is considered practically insignificant from 4000 to 6000 waves. Therefore, since the erosion and reshaping of the RMB profile surpassed 90% of the absolute limit (6000 waves) when 3000 waves hit the structure section, the time at which 3000 waves were hit is considered as the equilibrium time, with the 3000 waves taken to be the constant value in physical models. After the stones of the armor layer started to fall and the breakwater section initially reshaped (1000 waves), the wall slope becomes milder upon encountering with remaining waves. Profile change and rock fall gradually led to more surface contact and erosion in the wave energy absorption process resulting in increased wave energy absorption and reduced reflection coefficient of the structure. As Figure 11 shows, the reshaped profiles are influenced by incident waves for a fixed combination of wave height and period. Figure 12 shows the variation of the damage parameter along with the number of waves radiated.

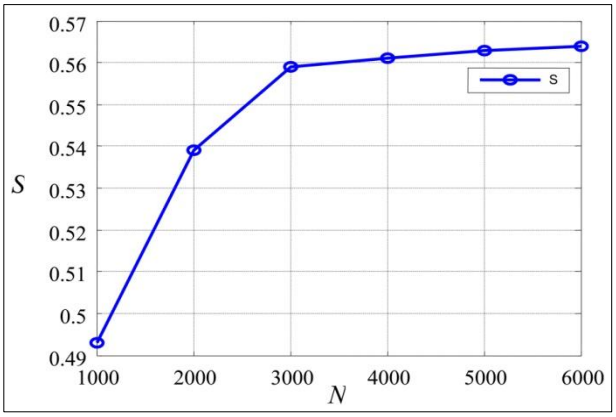

Figure 12. Damage parameter variations with different number of waves

Waves with 9, 12, and 15 cm height were generated by a paddle towards the RMB under a constant period (1 second) to study the effect of different wave heights on the erosion rate of the structure. The erosion rate and the profile reshaping were logged during the effective storm (3000 waves). Figure 13 plots the (non-dimensional) damage parameter against the non-dimensional wave height selected from among the numbers $\frac{H}{g.T^2}$, $\frac{H}{d}$ and $\frac{H}{H_{max}}$ (H: wave height, d: water depth, g: gravitational acceleration and T: wave period). This parameter was selected because the period is fixed due to the limited number of tests, so the choice of T could not be logical. Also, the number of wave chosen heights was 3; the maximum selection of the values could not generalize the height of multiple waves. The relationship between non-dimensional wave height and damage parameter was calculated from a linear fit with a regression coefficient of 0.99, as$S = 1.936(\frac{H}{d}) - 0.363$. Due to the low number of

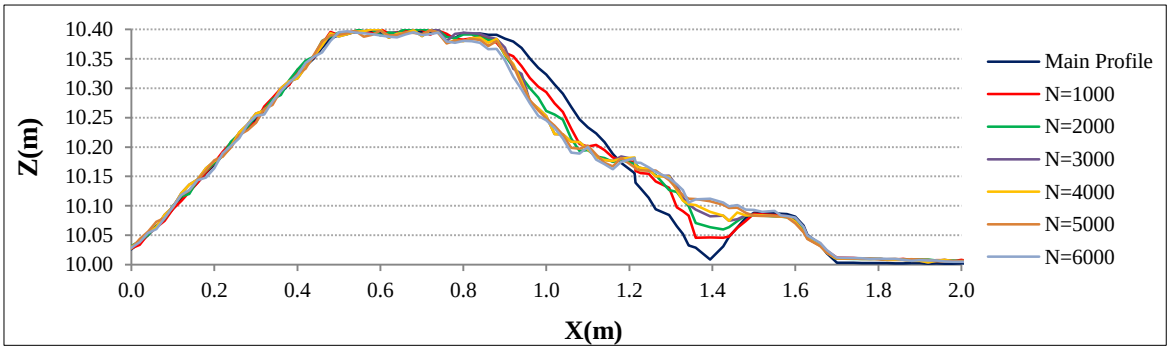

Figure 11. Comparison of the final profile reshaping of RMB under wave tests

points, this equation could not be generally used, as it was merely a preliminary estimation. Table 4 illustrates the numbers of relative wave height (wave height over water depth) and the damage parameter. As shown, the damage parameter increased by 39.12, and 44.44%, respectively, by increasing the relative wave height from 0.36 to 0.48 and 0.6. At a wave height of 15 cm, wave overflow from the breakwater was noticeable; thus, the wave height of 12 cm was used in physical models.

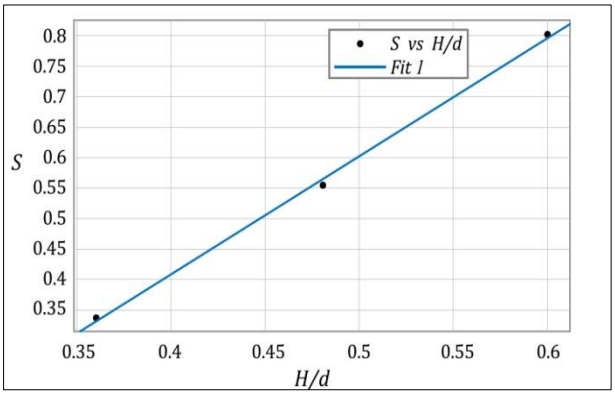

Figure 13. Variation of Damage parameter with wave height

Table 4. Relative wave height and damage parameter

H /d	0.36	0.48	0.60
S	0.3384	0.5560	0.8031

According to our analysis, as a parameter influencing the RMB stability, the wave period verified that erosion, at a constant wave height, increased by increasing wave period. Table 5 shows the relative wave period numbers (period over the maximum period) and damage parameters. These numbers indicate that as the relative wave period grows from 0.6 to 0.8 and 1, damage parameters increased by 22.94 and 28.26%. Thus, increasing the period would increase the damage parameter; nonetheless, increasing the wave height would have a more significant effect. In the wave period of 0.9 seconds, the wave steepness was high; it was sometimes noted that the wave would break before the wave strike the breakwater; whereas for the wave period of 1.5 seconds, the number of incident waves would decrease at a certain time. Consequently, the wave period of 1.2 cm was used in physical models.

Table 5. Relative wave period and damage parameter

T/T_{max}	0.6	0.8	1
S	0.4284	0.5560	0.7131

3.4. Physical models

Tests performed in the research are shown in Table 6.

Table 6. Performed tests

Test	RMB arrangement modes with obstacle and wave barrier
RB	RMB without obstacle and wave barrier
RBS	RMB with connected obstacle without wave barrier
RBF	RMB with wave barrier at 50 cm without obstacle
RBSF	RMB with connected obstacle and wave barrier at 50 cm

Figure 14 shows the reshaped profile of the RMB at each transversal section for the RBSF experiment altogether. Imaging results provide a 3D reshaping; besides, by sectioning each image, the eroded area (A_e) and the damage parameter are determined. Figure 15 compares the reshaped RMB profile in all test conditions. Table 7 demonstrates damage parameters in sections, height, period, and the number of waves calculated based on the experiments. In this table, H_{wm} is the wave height defined for the wavemaker, H_s, significant wave height taken from the water surface, T_{wm}, wave period specified for the wave maker, T_s, significant wave period taken from the water surface, N, the number of waves expected and N_{pr} the number of waves taken from the water surface. As Table 7 shows, the damage parameter of the RMB under random waves is 1.116. As shown in the table, the highest damage parameter pertained to the 20-cm section of the wall due to the wave behavior's complexity when hitting the breakwater, and waves also causing lateral motion upon hitting the coarse armor layer rocks. Moreover, due to the flow turbulence in this area, irregular motions are noted in the armor layer; thus, the accurate estimation is not possible by simply selecting a breakwater section for studying the stability, and more sections should be considered for a better assessment.

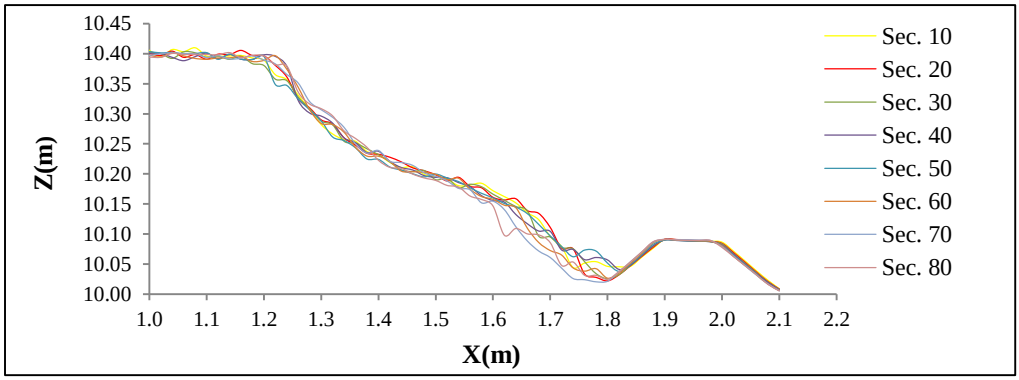

Figure 14. Reshaped RMB profile at each transversal section

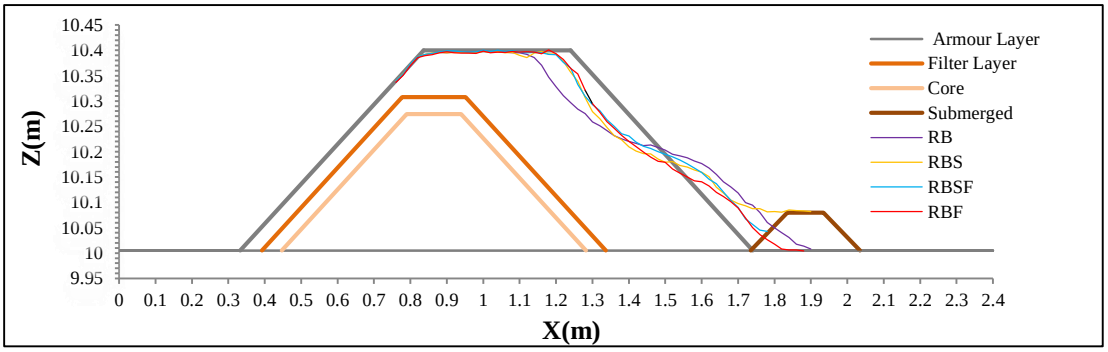

Figure 15. Reshaped RMB profiles in all tests

Table 7. Damage parameter in sections, height, period, and number of waves calculated in tests

	H (cm)		T (s)		N		S									
	H_{wm}	H_s	T_{wm}	T_s	N_0	N_{pr}	S_{10}	S_{20}	S_{30}	S_{40}	S_{50}	S_{60}	S_{70}	S_{80}	S_{max}	$S_{min(Final)}$
RB	12	11.52	1	0.95	3000	2783	1.033	**1.116**	1.075	1.099	1.048	1.014	1.017	0.959	**1.116**	
RBS	12	11.29	1	0.96	3000	2953	0.626	0.574	0.572	**0.701**	0.699	0.698	0.660	0.516	**0.701**	
RBF	12	11.29	1	0.94	3000	2709	0.549	0.629	0.667	0.628	0.601	0.576	**0.735**	0.503	**0.735**	**0.538**
RBSF	12	11.59	1	0.97	3000	2787	0.502	0.486	0.443	0.485	0.472	**0.538**	0.433	0.480	**0.538**	

As seen in table 7, the damage parameter was reduced by applying the obstacle to 0.701 (i.e., 37.19%), while the wave barrier reduced the damage parameter to 0.735 (i.e., 34.14%). Thus, the obstacle has outperformed the wave barrier. Using the obstacle with the wave barrier simultaneously reduced the damage parameter by 51.79%. Physically, it can be assumed that support was established for the breakwater when using the obstacle attached to the structure, which was effective against slides and overturning, with some of the eroded segments hitting it and stopping there. The simultaneous use of the obstacle and the wave barrier results in the highest efficiency, with the reduced-energy wave hitting the existing RMB with the obstacle. Seemingly, a reduced damage parameter by 51.79% would reduce RMB dimensions, significantly reducing the costs.

4. Conclusion

Based on the results of this study, the following conclusions have been drawn regarding the effect of a submerged obstacle and floating wave barrier in front of RMB diminishing the damage parameter:

- Using close-range photogrammetric imaging and developing 3D integrated models of breakwater profile changes has been an effective method for estimating the damage parameter in RMBs.
- Tests showed that the maximum profile change (over 50%) happened when the first 1000 waves hit. The erosion of the armor layer followed an increasing trend of up to 3000 waves, followed by the erosion pace between 3000 and 4000 waves decreasing. Besides, the erosion was found to be practically insignificant from 4000 to 6000 waves.
- Since the erosion and the breakwater profile change surpass over 90% of the absolute limit when 3000 waves hit the structure, increasing the wave height would increase the damage parameter. According to test results, damage parameters increase by 39.12 and 44.44%, respectively, by increasing the relative wave height from 0.36 to 0.48 and 0.6.
- In addition, increasing the period would increase the damage parameter; as the relative wave period expands from 0.6 to 0.8 and from 0.8 to 1, the damage parameter increase by 22.94 and 28.26%, respectively.
- Based on the results, the damage in transversal sections is different, and the middle band cannot be suggested for the stability study.
- Using the obstacle reduces the damage parameter to 0.701 (i.e., 37.19%), while the wave barrier reduces this parameter to 0.735 (i.e., 34.14%).
- The simultaneous use of the obstacle and the wave barrier results in the highest efficiency. Obviously, a reduced damage parameter by 51.79% would reduce RMB dimensions, significantly reducing the costs.
- Continuing studies of this research and future suggestions, changes in other parameters such as the RMB dimensions, the submerged obstacle dimensions, or the distance of the floating barrier can be examined.

5. References

[1] Khosravi Babadi, M., Golshani, A., Ghanei Ardakani, A. and Karami Matin, A., (2017), *Design principles of breakwaters*, Marine Industries Organization, p.17-23-42-111.

[2] Ghanbarian, M., (2010), *Rubble mound breakwaters (Vol.1: Types of breakwaters, principles, and overview*, Khatam al Anbiya Construction Headquarter, p.15-19. (In Persian)

[3] Sayao, O. and Da Silva R. F., (2016), *Analysis of rubble mound breakwater damage: Case study of existing breakwater rehabilitation*, IX Pinac Copedec Conference.

[4] Lamberti, A., Tomasicchio, G.R. and Guiducci, F., (1994), *Reshaping breakwaters in deep and shallow water conditions*, Proceeding of 24th International Conference on Coastal Engineering, Kobe, Japan. ASCE. p.1343-1358.

[5] Mousavi, Sh., (2010), *Rubble mound breakwaters (Vol.2: Design of rubble mound breakwaters*, Khatam al Anbiya Construction Headquarter, p.15-19-93-100-105. (In Persian)

[6] Campos, A., Castillo, C. and Sanchez, R.M., (2020), *Damage in rubble mound breakwaters. Part I: Historical review of damage models*, Journal of Marine Science and Engineering, Vol.8(5):317.

[7] Sayao, O., (1998), *On the profile reshaping of berm breakwaters*, Coastal structures, Vol.99, p.224-265.

[8] Rao, S. and Pramod, rao, B., (2003), *Stability of berm breakwater with reduced armour stone weight*, Ocean Engineering, Vol.31, p.1577-1589.

[9] Panagiota, G., Christos, M., and Panayotis, P., (2018), *Optimized reliability based upgrading of rubble mound breakwaters in a changing climate*, Journal of Marine Science and Engineering, 6(3):92.

[10] Janardhan, P., Harish, N., Rao, S. and Shirlal, K.G., (2015), *Performance of variable selection method for the damage level prediction of reshaped berm breakwater*, ICWRCOE 2015. Aquatic Procedia Vol.4, p.302- 307.

[11] Twu, S.W., Liu, C.C. and Hsu, W.H., (2001), *Wave damping characteristics of deeply submerged breakwaters*, ASCE Journal of Waterway, Port, Coastal, and Ocean Engineering Vol.127 (2), p.97–105.

[12] Neves, A.C., Veloso Gomes, F.and Taveira Pinto, F., (2007), *Analysis of the wave-flow interaction with submerged breakwaters*. WIT Transactions on Modelling and Simulation. Vol.46, p.147-154.

[13] Bungin, E.R., (2021), *The effect of square submerged breakwater on wave transmission in the coastal area*, AC2SET (2020), IOP Conference series: Materials Science and Engineering.

[14] Juhl, J. and Jensen, O. J., (1995), *Features of berm breakwaters and practical experience. Proceeding of the International Conference on Coastal and port engineering in developing countries*, R.J. Brazil. p.1307-1320.

[15] Tulsi, K., and Phelp, D., (2009), *Monitoring and maintenance of breakwaters which protect port entrances*, proceeding of the 28th South African transport conference, p.317 – 325.

[16] Smith, D.A.Y., Warner, P.S. and Sorensen, R.M., (1996), *Submerged-crest breakwater design, advances in coastal structures and breakwaters*, Thomas Telford, London, p.208–219.

[17] Stefanutti Stocks Marine, (2015), *Rubble mound breakwater vs. tandem breakwater cost estimation. Cape Town*, Stefanutti Stocks Marine.

[18] He, F., Huang, Z. and Law, A.W., (2012), *Hydrodynamic performance of a rectangular floating breakwater with and without pneumatic chambers: An experimental study*, Ocean Engineering, Vol.51 (1), p.16-27.

[19] Jian Xu, T., Wang, X.R., Guo, W.J., Dong, .H. and Hou, H.M, (2020), *Numerical simulation of combined effect of pneumatic breakwater and submerged breakwater on wave damping*, Taylor and Francis: Ships and offshore structures.

[20] Qin, H., Mu, L., Tang, W. and Hu, Z., (2019), *Numerical study of the interaction between peregrine breather based freak waves and twin-plate breakwater*, Journal of Fluids and Structures, Vol.87, p.206-227.

[21] Quiroga, I., Vidal, C., Lara, J., Gonzalez, M. and Sainz, A., (2018), *Stability of rubble-mound breakwaters under tsunami first impact and overflow based on laboratory experiments*, Coastal Engineering, Vol.135, p.39-54.

[22] Van der Meer, J.W., (1993), *Conceptual design of rubble mound breakwaters*, Delft Hydraulics, Report No. 483.

[23] Andersen, T.L., (2006). *Hydraulic response of rubble mound breakwaters (scale effects-berm breakwaters)*, University of Alborg, Denmark.

[24] Burcharth, H.F., (1993), *Design of breakwaters*, Department of Civil Engineering, Alborg University Denmark.

[25] Ataie Ashtiani, B., (2006), *Coastal engineering (Coastal hydrodynamics)*, ACECR, Amirkabir University of Technology Branch, p.214-215-218. (In Persian)

[26] Vafaeipour Sorkhabi R, Naseri A (2015) *Experimental investigation of the interaction between vertical flexible seawall and random sea waves.* Journal of Advanced Defense Science and Technology 6(3): 155-162. (In Persian)